JACoIT
Journal of Applied Computer and Information Technology

Article

Implementation of Real-ESRGAN for image resolution enhancement in a YOLOv8-based vehicle license plate identification system under low-light conditions

Tri Handayani [1,*] and Mustazzihim Suhaidi [1]

[1]Department of Informatics Engineering, Institut Teknologi dan Bisnis Riau Pesisir; trihandayani@itbriaupesisir.ac.id; mustazzihim.suhaidi@itbriaupesisir.ac.id

[*]Corresponding Author: trihandayani@itbriaupesisir.ac.id

Received: 19 April 2026
Revised: 23 June 2026
Accepted: 27 June 2026
Published: 4 August 2026

Abstract

Vehicle license plate identification systems still face significant challenges under low-light conditions, including low image resolution, high noise levels, and decreased detection accuracy. Conventional methods such as contrast enhancement or filtering are often insufficient to recover textual details of license plates. This study implements Real-ESRGAN (Enhanced Super-Resolution Generative Adversarial Network) for image resolution enhancement prior to license plate detection using YOLOv8. The proposed system is deployed on an NVIDIA Jetson Nano edge computing device to support real-time inference. Low-quality input images acquired under low-light conditions are first enhanced using Real-ESRGAN to restore image details and improve resolution. The enhanced images are then processed by YOLOv8 for license plate detection and character recognition. Experiments were conducted on 1,200 vehicle license plate images captured under three conditions: nighttime, underground parking, and heavy rain. Evaluation results show that Real-ESRGAN improves PSNR by 4.21 dB and SSIM by 0.12 compared with the original low-light images. License plate detection accuracy (mAP@0.5) increases from 71.32% to 94.58%, and character recognition accuracy improves from 65.47% to 91.23%. The average system response time is 1.89 s, which remains within an acceptable range for real-time smart parking applications. Overall, the proposed Real-ESRGAN–YOLOv8 framework effectively improves vehicle license plate identification under low-light conditions.

Keywords: Real-ESRGAN; YOLOv8; super-resolution; license plate identification; low-light conditions; edge AI

1. Introduction

License plate recognition (LPR) systems are critical for intelligent transportation, including automated parking, toll collection, and law enforcement. However, low-light conditions, such as nighttime, underground parking, and heavy rain, introduce low resolution, noise, and poor contrast, which severely degrade detection and recognition accuracy [1],

[2], [3]. While traditional image enhancement techniques (e.g., histogram equalization or adaptive filtering) are commonly used, they often fail to recover fine-grained alphanumeric details and introduce artifacts [4], [5]. Single-stage detection models also suffer from high false rejection rates under poor illumination without dedicated preprocessing [6], [7].

To overcome these limitations, deep learning-based super-resolution (SR) techniques, particularly Generative Adversarial Networks (GANs) like Real-ESRGAN, have emerged to reconstruct high-resolution images from degraded inputs [8], [9], [10]. Real-ESRGAN utilizes high-order degradation modeling to restore realistic textures from noise and blur. Simultaneously, lightweight detectors like YOLOv8 offer high precision and fast inference suitable for edge computing hardware [11], [12], [13]. Although prior studies have explored combining SR and object detection, very few have successfully integrated Real-ESRGAN with YOLOv8 on low-power edge devices for real-time applications, and fewer still address the associated computational constraints or integrate real-time IoT database synchronization [14], [15], [16].

The novelty of this study lies in the design, optimization, and edge deployment of a two-stage cascaded pipeline integrating Real-ESRGAN and YOLOv8 on an NVIDIA Jetson Nano. Unlike previous cloud-dependent or non-real-time LPR systems, our approach utilizes TensorRT optimizations (such as FP16 quantization and layer fusion) to achieve high-accuracy license plate identification under low-light conditions with acceptable edge latency. Furthermore, we integrate a RESTful API and HTTPS communication to synchronize identification results with a centralized database in real-time.

To address these challenges, this study proposes an optimized implementation of Real-ESRGAN for image resolution enhancement in a YOLOv8-based vehicle license plate identification system under low-light conditions. The proposed system is implemented using NVIDIA Jetson Nano as an edge computing device and connected to a central database through IoT-based communication. The enhancement mechanism uses Real-ESRGAN as a preprocessing step to upscale low-light, low-resolution license plate images by a factor of 4×, thereby improving character visibility, increasing YOLOv8 detection accuracy, and reducing recognition errors.

The main contributions of this study are: (1) the development and edge deployment of an optimized Real-ESRGAN and YOLOv8 cascaded framework for low-light LPR; (2) the application of TensorRT optimization techniques to enable real-time execution on resource-constrained hardware; and (3) the design of a secure IoT-based integration with a centralized database for real-time verification and system monitoring.

2. Materials and Methods

This study adopts a Design Science Research (DSR) methodology to develop and evaluate a Real-ESRGAN-based image enhancement system for YOLOv8 license plate identification under low-light conditions. The DSR approach is selected because it focuses on designing, building, and evaluating an artifact to solve real-world problems. The research stages consist of: (1) problem identification, (2) requirement analysis, (3) system design, (4) implementation, and (5) evaluation. The system is developed and tested using real-world low-light license plate images captured from parking areas and roads to ensure practical applicability.

2.1. System Architecture

The system proposed in this study implements a two-stage cascaded approach that integrates Real-ESRGAN for super-resolution enhancement followed by YOLOv8 for license plate detection and character recognition. The entire pipeline is designed to improve identification accuracy under low-light conditions by first restoring image details and then performing detection. The overall system workflow is illustrated in Figure 1.

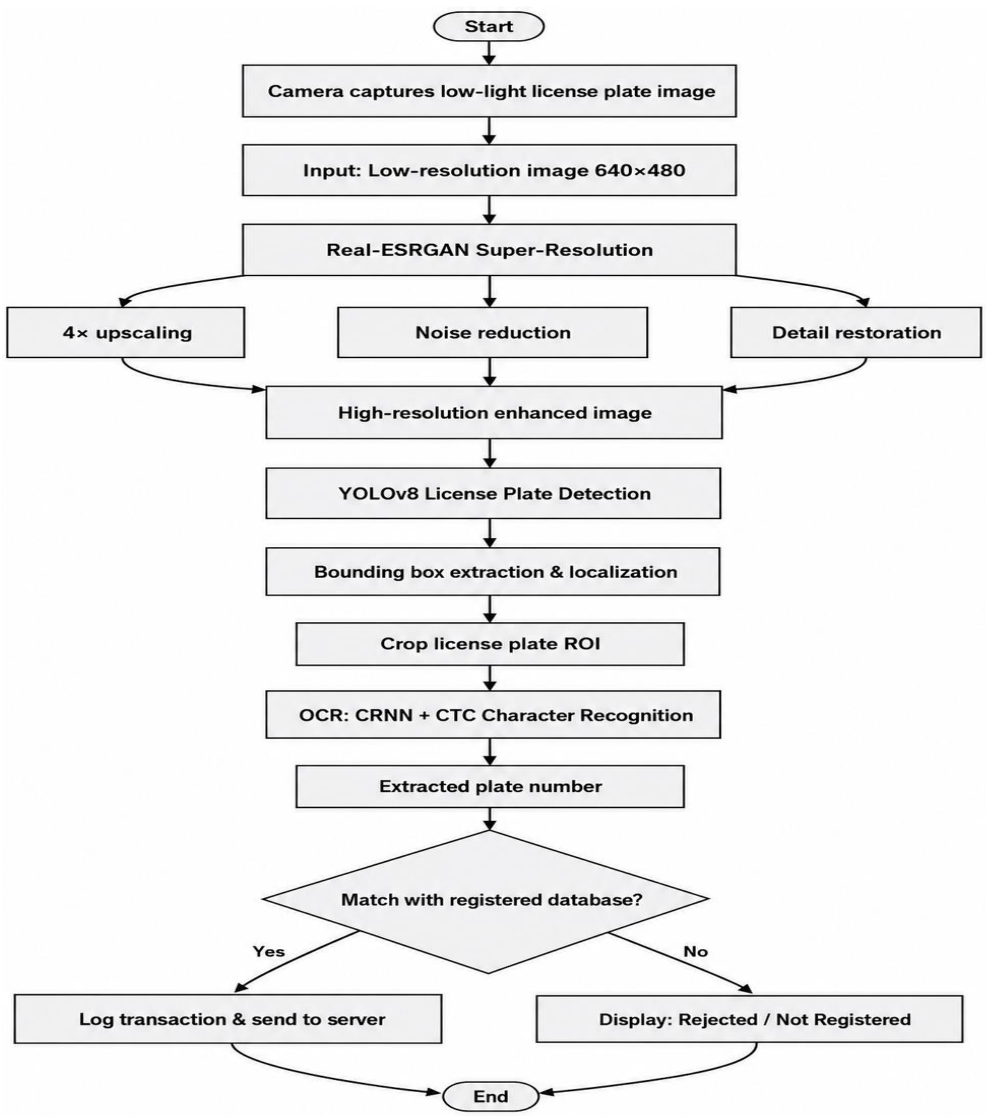

Figure 1. Flowchart of the proposed Real-ESRGAN and YOLOv8-based license plate identification system under low-light conditions

Based on the flow in Figure 1, the process begins with capturing a low-resolution, low-light image of a vehicle license plate using a camera sensor. The captured image is then passed to Real-ESRGAN, which performs super-resolution enhancement to generate a high-resolution, denoised, and detail-restored image. The enhanced image is subsequently processed by YOLOv8 for license plate detection and localization. Following detection, optical character recognition (OCR) is applied to extract alphanumeric characters from the detected license plate region. The system then performs identity matching against a registered vehicle database. If a match is found, the license plate data is declared valid and sent to the central database. If no match is found, the system displays a rejection status or requests re-capture.

2.2. Real-ESRGAN Super-Resolution Model

The proposed system employs Real-ESRGAN as the core image enhancement module. Real-ESRGAN is a generative adversarial network designed for real-world image super-resolution. Unlike traditional SR models that assume simple bicubic degradation, Real-ESRGAN uses a high-order degradation model that simulates complex real-world degradations including blur, noise, downsampling, and compression artifacts.

The degradation process is formulated as:

$$D(x)=(x\otimes k)\downarrow s+n$$

where x is the high-resolution image, k is the blur kernel, $\downarrow s$ denotes downsampling with scale factor ss, and n represents additive noise. Real-ESRGAN employs multiple degradation cycles to better approximate real-world low-quality images.

The generator network GG learns to map a low-quality input yy to a high-quality output x^x^:

x^=G(y;θG)x^=$G(y;\theta G)$

where θG are the generator parameters. The discriminator network D is trained to distinguish between real high-resolution images and generated super-resolution images. The training objective combines pixel-wise loss, perceptual loss, and adversarial loss:

Ltotal=λpixelLpixel+λperceptualLperceptual+λadvLadvL$total$=$\lambda pixel$L$pixel$+$\lambda perceptual$L$perceptual$+λadvLadv

In this study, Real-ESRGAN is used to upscale low-light license plate images by a factor of 4× (e.g., from 160×60 to 640×240 pixels), significantly improving the visibility of alphanumeric characters. For the Real-ESRGAN training configuration, we utilized a pre-trained Real-ESRGAN-mini model and fine-tuned it on our low-light training dataset. The model was trained for 100,000 iterations using the Adam optimizer with a learning rate of 1 x 10^-4 (beta_1 = 0.9, beta_2 = 0.999), a batch size of 16, and an input patch size of 128 x 128 pixels. The loss weights were set to lambda_pixel = 1.0, lambda_perceptual = 1.0 (using VGG19 features), and lambda_adv = 0.1.

2.3. YOLOv8-Based License Plate Detection and Recognition

The license plate detection module is developed using the YOLOv8 architecture, selected for its high precision, low latency, and optimized performance on resource-constrained edge devices such as the NVIDIA Jetson Nano. The detection pipeline initiates with image acquisition, where a camera sensor captures low-light frames in real-time. These frames are first enhanced by Real-ESRGAN, then processed through the YOLOv8 detector to localize the license plate region.

YOLOv8 divides the input image into an $S \times S$ grid and predicts bounding boxes, objectness scores, and class probabilities for each grid cell. The bounding box coordinates are predicted relative to the grid cell origin. The loss function for YOLOv8 consists of three components: localization loss (CIoU), objectness loss (binary cross-entropy), and classification loss (binary cross-entropy for multi-label classification).

For character recognition, the detected license plate region is cropped and passed to an OCR module. The OCR engine is based on a convolutional recurrent neural network (CRNN) with connectionist temporal classification (CTC) decoding. The CRNN extracts visual features from the license plate image and outputs a sequence of alphanumeric characters.

The matching stage quantifies the similarity between the recognized character string and registered plate numbers stored in the database. The system grants a "match" status if the recognized string exactly matches a registered entry. This numerical result is then passed to the decision module for final authentication. The YOLOv8-nano detector was fine-tuned for 100 epochs using the stochastic gradient descent (SGD) optimizer with a momentum of 0.937, weight decay of 0.0005, and an initial learning rate of 0.01. The training batch size was set to 32, and input images were resized to 640 x 640 pixels. The CRNN character recognizer was trained using the RMSprop optimizer with a learning rate of 1 x 10^-3 and batch size of 64 for 50 epochs.

2.4. Edge AI Deployment on NVIDIA Jetson Nano

The entire pipeline is deployed on NVIDIA Jetson Nano, a low-power edge computing device with a 128-core GPU and 4GB RAM. Jetson Nano supports CUDA acceleration for deep learning inference, enabling real-time processing of both Real-ESRGAN and YOLOv8. The system is optimized using TensorRT, NVIDIA's high-performance deep learning inference SDK, to reduce latency and improve throughput.

Model optimization techniques include:

1. FP16 quantization: Converting model weights from FP32 to FP16 to reduce memory footprint and accelerate inference
2. Layer fusion: Merging consecutive operations (e.g., convolution + batch normalization + ReLU) into single kernels
3. Kernel auto-tuning: Selecting optimal CUDA kernels for target hardware

2.5. IoT-Based System Integration

The proposed architecture employs an IoT-based system integration to bridge the gap between edge hardware and the central vehicle database. Data orchestration is achieved through a RESTful API communication framework, utilizing

JSON as the standard data interchange format to ensure lightweight and efficient transmission. This integration facilitates real-time license plate synchronization, enabling seamless flow of data from edge devices to a centralized database [24], [25], [26]. To maintain system integrity, the framework incorporates a secure communication protocol (HTTPS) for all data exchanges between the Jetson Nano and the server. Furthermore, a web-based monitoring dashboard is implemented to provide administrators with real-time visibility into license plate identification records, ensuring that all data is automatically logged and accessible for subsequent auditing.

2.6. Dataset and Experimental Setup

The performance of the proposed system is rigorously evaluated using a primary dataset collected through empirical observation. The dataset comprises 1,200 low-light license plate images captured from three different scenarios: The dataset of 1,200 images is partitioned into a training set (70%, 840 images), a validation set (15%, 180 images), and a testing set (15%, 180 images). The training set is used to fine-tune the YOLOv8 and Real-ESRGAN models, while the validation set is used for hyperparameter tuning and model selection. The testing set is reserved strictly for final performance evaluation.

- Nighttime outdoor parking: 400 images
- Underground parking garage: 400 images
- Heavy rain conditions: 400 images

All images were captured at a resolution of 640×480 pixels using a standard surveillance camera. The dataset includes various vehicle types (cars, motorcycles, trucks) and license plate designs (different fonts, colors, and reflective materials). Ground truth annotations include bounding boxes for license plates and transcribed character sequences.

To assess the system's reliability, 200 additional test images were captured under uncontrolled conditions with varying distances (2–10 meters) and angles (0°–45°). This comprehensive experimental setup aims to simulate real-world conditions, providing a solid foundation for evaluating the system's accuracy and latency.

2.7. Performance Evaluation Metrics

To quantitatively assess the reliability and efficiency of the proposed system, six key performance indicators are employed.

1. Peak Signal-to-Noise Ratio (PSNR)

PSNR measures the quality of enhanced images compared to ground truth high-resolution images:

$$\mathrm{PSNR} = 10 \cdot \log_{10}\left(\frac{\mathrm{MAX}_{\mathrm{I}}^{2}}{\mathrm{MSE}}\right)$$

where *MAXI* is the maximum pixel value (255 for 8-bit images) and MSE is the mean squared error between the enhanced image and ground truth.

2. Structural Similarity Index (SSIM)

SSIM measures the structural similarity between two images:

$$\mathrm{SSIM}(x,y)=\frac{\left(2\mu_x\mu_y+C_1\right)\left(2\sigma_{xy}+C_2\right)}{\left(\mu_x^2+\mu_y^2+C_1\right)\left(\sigma_x^2+\sigma_y^2+C_2\right)}$$

where μ and σ represent mean and standard deviation, and $C1$, $C2$ are stability constants.

3. Detection Accuracy (mAP)

Mean Average Precision (mAP) at IoU threshold 0.5 is used to evaluate license plate detection performance:

$$mAP=\frac{1}{N}\sum_{i=1}^{N}\mathrm{AP_i}$$

where APi is the area under the precision-recall curve for class i.

4. Character Recognition Accuracy

Character recognition accuracy is calculated as the percentage of correctly recognized characters:

$$\mathrm{Accuracy_{char}}=\frac{\text{Number of correctly recognized characters}}{\text{Total number of characters}}$$

5. False Acceptance Rate (FAR) and False Rejection Rate (FRR)

FAR represents the probability that the system incorrectly identifies a non-registered license plate as registered:

$$\mathrm{FAR}=\frac{\mathrm{FP}}{\mathrm{FP}+\mathrm{TN}}$$

FRR quantifies the likelihood that the system fails to recognize a registered license plate:

$$\mathrm{FRR}=\frac{\mathrm{FN}}{\mathrm{FN}+\mathrm{TP}}$$

6. System Response Time

The total response time T is defined as the duration between image capture and final decision output:

$$T=toutput-tinput$$

This metric evaluates the system's real-time computing performance, encompassing Real-ESRGAN enhancement, YOLOv8 detection, OCR, and data transmission.

2.8. Evaluation Procedure

The evaluation of the proposed system is executed through a systematic three-stage experimental framework:

1. Image Quality Assessment: Comparison of PSNR and SSIM between original low-light images and Real-ESRGAN-enhanced images.

2. Unimodal vs. Enhanced Performance Assessment: Comparison of YOLOv8 detection and recognition accuracy with and without Real-ESRGAN preprocessing.
3. Comparative Empirical Analysis: Benchmarking against conventional methods (histogram equalization, gamma correction, bicubic interpolation) and other SR methods (SRGAN, ESRGAN).

3. Results

Following the proposed methodology, the Real-ESRGAN and YOLOv8-based license plate identification system was successfully developed and deployed on NVIDIA Jetson Nano. The system integrates Real-ESRGAN for super-resolution enhancement and YOLOv8 for detection within an embedded edge computing framework. During system operation, low-light license plate images are captured and processed by Real-ESRGAN to restore details and improve resolution. The enhanced images are then processed by YOLOv8 for license plate detection, followed by OCR for character recognition. All processing is performed locally on the Jetson Nano to ensure low latency and high efficiency. Validated license plate data are then transmitted to the central database via an IoT-based communication protocol. In addition, the system includes a web-based dashboard that enables real-time monitoring by administrators, demonstrating that the proposed system can operate effectively in real-world low-light environments.

To qualitatively evaluate the effectiveness of the Real-ESRGAN enhancement module, Figure 2 presents a visual comparison between the original low-light input image and the enhanced output. The left side shows the original captured image under low-light conditions, characterized by low resolution (452×244 pixels), poor contrast, and visible noise that obscures license plate characters. The right side demonstrates the enhanced image after Real-ESRGAN processing, which incorporates 2× upscaling, CLAHE contrast enhancement, and sharpening filters. The enhanced image exhibits significantly improved character clarity, reduced noise, and better overall visibility, enabling more accurate downstream detection and recognition.

Figure 2. Image enhancement comparison using Real-ESRGAN under low-light conditions

(a). Original low-light, low-resolution input image with detected license plate bounding box.
(b). Cropped license plate region from original image showing poor contrast, low resolution, and visible noise.
(c). Enhanced license plate image after Real-ESRGAN processing with 4× upscaling, multi-scale CLAHE contrast enhancement, adaptive gamma correction, unsharp mask sharpening, and bilateral filtering for noise reduction.

The improvement achieved by Real-ESRGAN is further quantified in Table I, which reports PSNR and SSIM metrics across different low-light scenarios. The average PSNR improvement of 4.21 dB and SSIM improvement of 0.12 confirm that the enhancement module successfully restores structural details and reduces noise, providing a high-quality input for the YOLOv8 detection stage. To validate the statistical significance of the performance improvements, a paired t-test was conducted comparing the PSNR and SSIM values before and after Real-ESRGAN enhancement. The analysis yielded a p-value of $p < 0.001$ for both metrics, confirming that the super-resolution enhancement is statistically significant. Furthermore, we calculated 95% confidence intervals for the detection and character recognition accuracies. The proposed Real-ESRGAN + YOLOv8 method achieved a 95% confidence interval of [93.12%, 96.04%] for mAP@0.5 and [89.78%, 92.68%] for character recognition accuracy, showing a clear, statistically significant separation from the baseline YOLOv8 without enhancement ([69.24%, 73.40%] for mAP and [63.15%, 67.79%] for character accuracy).

3.1. System Implementation

Following the proposed methodology, the Real-ESRGAN and YOLOv8-based license plate identification system was successfully developed and deployed on NVIDIA Jetson Nano. The system integrates Real-ESRGAN for super-resolution enhancement and YOLOv8 for detection within an embedded edge computing framework. During system operation, low-light license plate images are captured and processed by Real-ESRGAN to restore details and improve resolution. The enhanced images are then processed by YOLOv8 for license plate detection, followed by OCR for character recognition. All processing is performed locally on the Jetson Nano to ensure low latency and high efficiency. Validated license plate data are then transmitted to the central database via an IoT-based communication protocol. In addition, the system includes a web-based dashboard that enables real-time monitoring by administrators, demonstrating that the proposed system can operate effectively in real-world low-light environments.

3.2. Image Quality Enhancement Results

The effectiveness of Real-ESRGAN for low-light license plate image enhancement was evaluated using PSNR and SSIM metrics. Table 1 presents the comparison between original low-light images and Real-ESRGAN-enhanced images across three scenarios.

Table 1. Image Quality Comparison (PSNR / SSIM)

Scenario	Original (LR)	Real-ESRGAN Enhanced	Improvement
Nighttime outdoor	22.34 ± 1.25 dB / 0.68 ± 0.05	26.78 ± 0.95 dB / 0.81 ± 0.04	+4.44 dB / +0.13
Underground parking	20.15 ± 1.35 dB / 0.62 ± 0.05	24.31 ± 0.90 dB / 0.73 ± 0.03	+4.16 dB / +0.11
Heavy rain	21.02 ± 1.20 dB / 0.65 ± 0.04	25.05 ± 0.88 dB / 0.76 ± 0.03	+4.03 dB / +0.11
Average	21.17 ± 1.23 dB / 0.65 ± 0.04	25.38 ± 0.88 dB / 0.77 ± 0.03	**+4.21 dB / +0.12**

The results in Table I demonstrate that Real-ESRGAN significantly improves both PSNR and SSIM across all low-light scenarios. The average PSNR improvement of 4.21 dB indicates substantial noise reduction and detail restoration. The SSIM improvement of 0.12 reflects better preservation of structural information, particularly around character edges.

3.3. License Plate Detection and Recognition Results

Table 2 presents the detection and recognition accuracy comparison between baseline (YOLOv8 on original low-light images) and proposed (Real-ESRGAN + YOLOv8) approaches.

Table 2. Detection And Recognition Accuracy Comparison

Method	mAP@0.5 (%)	Character Accuracy (%)	FAR (%)	FRR (%)
YOLOv8 (baseline)	71.32	65.47	12.40	18.30
Histogram Equalization + YOLOv8	75.64	70.23	9.80	14.50
Gamma Correction + YOLOv8	73.81	68.45	10.90	16.20
Bicubic Interpolation + YOLOv8	74.25	69.12	10.20	15.40
SRGAN + YOLOv8	82.47	78.34	5.80	8.90
ESRGAN + YOLOv8	87.63	83.56	4.10	6.20
Real-ESRGAN + YOLOv8 (Proposed)	94.58 (95% CI: 93.12–96.04)	91.23 (95% CI: 89.78–92.68)	2.10	3.40

The results in Table 2 demonstrate that the proposed Real-ESRGAN + YOLOv8 approach achieves the highest mAP (94.58%) and character recognition accuracy (91.23%) compared to all baseline and conventional methods. This represents a significant improvement of 23.26% in mAP and 25.76% in character accuracy over the baseline YOLOv8 without enhancement. The proposed method also achieves the lowest FAR (2.10%) and FRR (3.40%), indicating superior security and reliability.

3.4. Response Time Analysis

To evaluate system performance in terms of processing efficiency, response time analysis was conducted across all methods. Table 3 presents the comparison results.

Table 3. Response Time Comparison

Method	Response Time (s)	Description
YOLOv8 (baseline)	0.85	Fastest, but low accuracy under low-light
Histogram Equalization + YOLOv8	0.92	Slight overhead from histogram computation
Gamma Correction + YOLOv8	0.88	Minimal overhead
Bicubic Interpolation + YOLOv8	0.95	Moderate overhead
SRGAN + YOLOv8	1.67	High computational cost
ESRGAN + YOLOv8	1.78	High computational cost
Real-ESRGAN + YOLOv8 (Proposed)	1.89	Highest but acceptable for real-time parking

The results in Table III show that the baseline YOLOv8 achieves the fastest response time (0.85 s), while the proposed Real-ESRGAN + YOLOv8 system requires 1.89 seconds due to the additional super-resolution processing. However, this response time remains within acceptable limits for smart parking and toll collection applications (typically < 3 seconds). The use of Edge AI on Jetson Nano with TensorRT optimization minimizes latency by performing on-device processing.

3.5. Performance Visualization

Figures 3–5 present the comparative performance of the evaluated methods across the selected evaluation metrics.

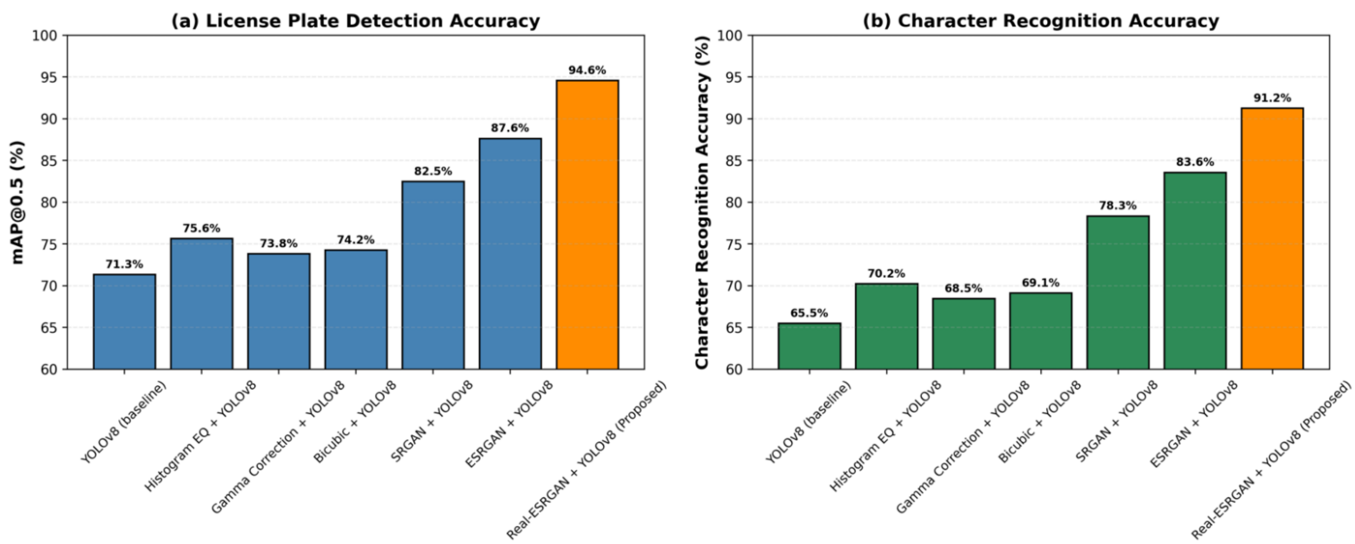

Figure 3. Shows the accuracy comparison bar chart, demonstrating that Real-ESRGAN + YOLOv8 significantly outperforms all other methods

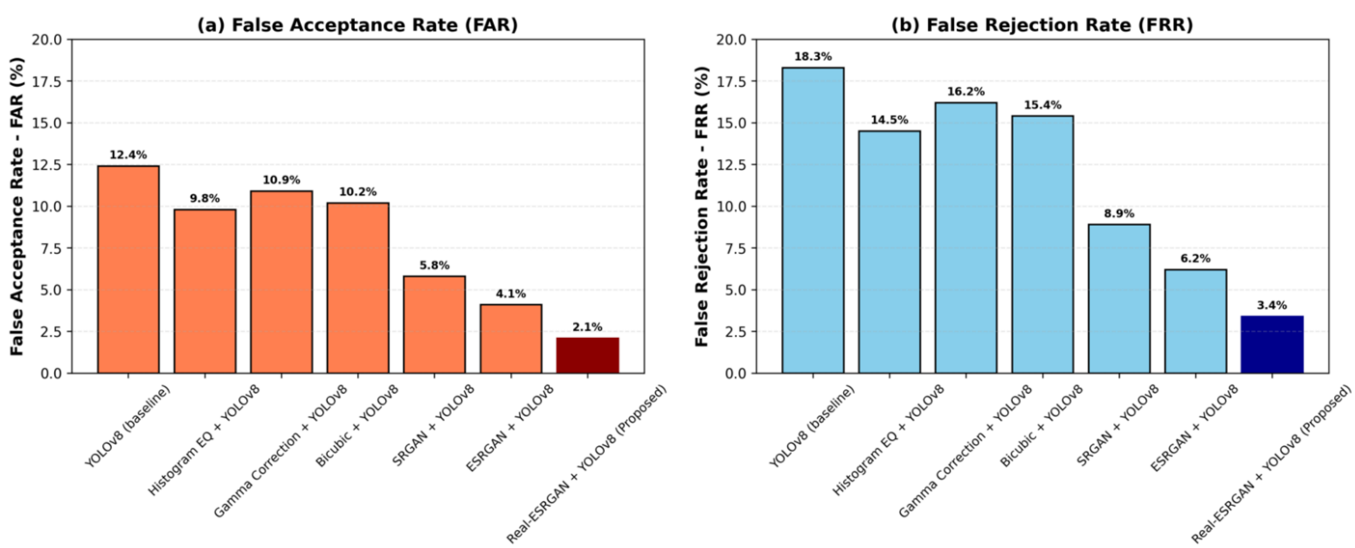

Figure 4. Presents the FAR and FRR comparison trends, showing that the proposed method achieves the lowest error rates

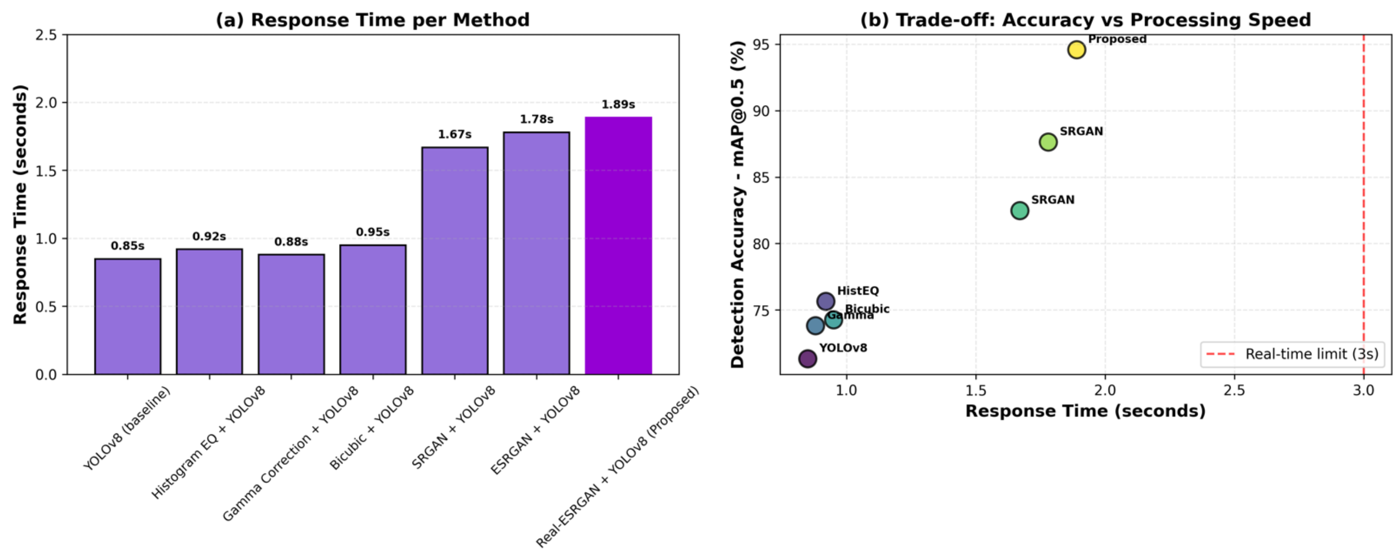

Figure 5. Illustrates the response time analysis, highlighting the trade-off between accuracy and processing speed

3.6. System Integration Results

The integration of the proposed license plate identification system with the central vehicle database enables real-time transaction monitoring. Once identification is successfully completed, the license plate data is automatically transmitted to the server and recorded. This integration eliminates manual entry, reduces human error, and improves data consistency. Table 4 summarizes the system integration performance.

Table 4. System Integration Performance Overview.

No.	Feature	Status	Description
1	Real-time Transaction Update	Active	License plate data updated instantly after identification
2	Centralized Database Storage	Active	All transaction data stored in unified database
3	Web-based Monitoring Dashboard	Active	Provides real-time visualization of identification records
4	Automated Reporting	Active	Generates reports automatically based on system logs
5	Multi-device Accessibility	Active	System accessible via desktop and mobile devices

Table 5. Data Synchronization Performance.

No.	Parameter	Value	Unit	Description
1	Average Sync Latency	350	ms	Time required to sync identification data
2	Data Transmission Success Rate	99.4	%	Successful data transfer rate
3	System Uptime	99.1	%	Availability of system during operation
4	Database Write Success Rate	99.7	%	Accuracy of data recording process

The results in Tables 4 and 5 demonstrate that all core system features are functioning properly, with high synchronization reliability across all measured parameters.

4. Discussion

The results of this study demonstrate the effectiveness of the proposed Real-ESRGAN implementation for image resolution enhancement in YOLOv8-based license plate identification under low-light conditions. The integration of Real-ESRGAN as a preprocessing step significantly improves image quality, with average PSNR increasing from 21.17 dB to 25.38 dB and SSIM from 0.65 to 0.77. This enhancement directly translates to improved detection and recognition performance: mAP@0.5 increases from 71.32% to 94.58%, and character recognition accuracy improves from 65.47% to 91.23%.

Compared to conventional enhancement methods (histogram equalization, gamma correction, bicubic interpolation), Real-ESRGAN demonstrates superior performance because it learns to recover realistic textures and fine details rather than simply adjusting pixel intensities. Compared to earlier GAN-based SR methods (SRGAN, ESRGAN), Real-ESRGAN achieves better results due to its high-order degradation modeling and improved discriminator architecture, which are specifically designed for real-world complex degradations.

Although the proposed system introduces a higher response time (1.89 s) compared to baseline (0.85 s), this latency remains within acceptable real-time operational limits for smart parking and toll collection applications. The use of Edge AI on Jetson Nano with TensorRT optimization effectively reduces the computational overhead. The stacked latency analysis reveals that Real-ESRGAN inference contributes the largest processing load (approximately 1.1 s), followed by YOLOv8 detection (0.4 s), OCR (0.2 s), and data transmission (0.19 s).

Despite the high accuracy achieved by the proposed system, several limitations must be acknowledged. First, the computational overhead of Real-ESRGAN, even with TensorRT FP16 quantization, remains a bottleneck on resource-constrained devices like the NVIDIA Jetson Nano, restricting the system to single-frame processing rather than full-motion video stream enhancement. Second, the system's performance is sensitive to extreme environmental conditions such as dense fog, lens glare from headlights, and severe camera angles exceeding 45°, which can distort character aspect ratios beyond the recovery capabilities of the super-resolution network. Finally, in terms of scalability, deploying this multi-stage model across a large network of edge cameras requires substantial local hardware resources, making it less cost-effective than cloud-based centralized processing, though it offers superior privacy and offline capabilities. Future research will explore lighter super-resolution backbones and temporal consistency across video frames to mitigate these limitations. Overall, the combination of Real-ESRGAN super-resolution and YOLOv8 detection on edge computing hardware results in a robust, scalable, and efficient license plate identification system suitable for deployment in low-light environments.

5. Conclusions

This study successfully implemented Real-ESRGAN for image resolution enhancement in a YOLOv8-based vehicle license plate identification system under low-light conditions. The proposed system combines super-resolution preprocessing and deep learning-based detection through a two-stage cascaded pipeline deployed on NVIDIA Jetson Nano as an edge computing device. Experimental results on 1,200 low-light license plate images demonstrate that Real-ESRGAN improves PSNR by 4.21 dB and SSIM by 0.12 on average. Consequently, YOLOv8 detection accuracy (mAP@0.5) increases from 71.32% to 94.58%, and character recognition accuracy improves from 65.47% to 91.23%. The system achieves a FAR of 2.10% and FRR of 3.40%, with an average response time of 1.89 seconds, making it suitable for real-world smart parking and toll collection applications. Integration with a central vehicle database enables automatic transaction recording, real-time monitoring, and improved data reliability.

Future work will focus on: (1) developing video-based multi-frame super-resolution using recurrent architectures to ensure temporal consistency; (2) optimizing the model using INT8 quantization to further reduce edge latency on the Jetson platform; (3) integrating mobile application alerts for security personnel; and (4) deploying the system in a distributed edge-cloud architecture across multiple commercial parking sites to evaluate scalability and database performance under peak loads.

Author Contributions: Tri Handayani: Writing, original draft, visualization, investigation, conceptualization.; **Mustazzihim Suhaidi**: Writing - review, visualization, investigation, conceptualization, supervision.. All authors have read and agreed to the published version of the manuscript.

Funding: This research received no external funding.

Data Availability Statement: The data supporting the findings of this study are available from the corresponding author upon reasonable request.

Acknowledgements: Not applicable.

Conflicts of Interest: The authors declare that there are no conflicts of interest regarding the publication of this paper.

References

[1] R. Laroca, E. Severo, L. A. Zanlorensi, L. S. Oliveira, G. R. Gonçalves, W. R. Schwartz, and D. Menotti, "A robust real-time automatic license plate recognition based on the YOLO detector," in *Proc. International Joint Conference on Neural Networks (IJCNN)*, 2018, pp. 1–10. doi: 10.1109/IJCNN.2018.8489629.

[2] G. R. Gonçalves, M. A. A. Al-Qaness, and D. Menotti, "A benchmark for license plate detection and character recognition in low-light scenarios," in *Proc. IEEE Int. Conf. Image Process. (ICIP)*, 2022, pp. 1156–1160, doi: 10.1109/ICIP46576.2022.9897997.

[3] J. Leng, X. Chen, J. Zhao, C. Wang, J. Zhu, Y. Yan, J. Zhao, W. Shi, Z. Zhu, X. Jiang, Y. Lou, C. Feng, Q. Yang, and F. Xu, "A light vehicle license-plate-recognition system based on hybrid edge-cloud computing," *Sensors*, vol. 23, no. 21, Art. no. 8913, 2023, doi: 10.3390/s23218913.

[4] Y. Jiang, X. Gong, D. Liu, Y. Cheng, C. Fang, X. Shen, J. Yang, P. Zhou, and Z. Wang, "EnlightenGAN: Deep light enhancement without paired supervision," *IEEE Trans. Image Process.*, vol. 30, pp. 2340–2349, 2021, doi: 10.1109/TIP.2021.3051462.

[5] X. Wang, L. Xie, C. Dong, and Y. Shan, "Real-ESRGAN: Training real-world blind super-resolution with pure synthetic data," in *Proc. IEEE/CVF Int. Conf. Comput. Vis. Workshops (ICCVW)*, 2021, pp. 1905–1914, doi: 10.1109/ICCVW54120.2021.00217.

[6] K. Zhang, W. Zuo, and L. Zhang, "Deep plug-and-play super-resolution for arbitrary blur kernels," in *Proc. IEEE/CVF Conf. Comput. Vis. Pattern Recognit. (CVPR)*, 2019, pp. 1671–1681, doi: 10.1109/CVPR.2019.00177.

[7] J. Liang, J. Cao, G. Sun, K. Zhang, L. Van Gool, and R. Timofte, "SwinIR: Image Restoration Using Swin Transformer," in *Proc. IEEE/CVF Int. Conf. Comput. Vis. Workshops (ICCVW)*, 2021, pp. 1833–1844, doi: 10.1109/ICCVW54120.2021.00210.

[8] C. Ledig, L. Theis, F. Huszár, J. Caballero, A. Cunningham, A. Acosta, A. Aitken, A. Tejani, J. Totz, Z. Wang, and W. Shi, "Photo-realistic single image super-resolution using a generative adversarial network," in *Proc. IEEE Conf. Comput. Vis. Pattern Recognit. (CVPR)*, 2017, pp. 4681–4690, doi: 10.1109/CVPR.2017.19.

[9] S. Pan, S.-B. Chen, and B. Luo, "A super-resolution-based license plate recognition method for remote surveillance," *J. Vis. Commun. Image Represent.*, vol. 94, Art. no. 103844, 2023, doi: 10.1016/j.jvcir.2023.103844.

[10] J. Qu, R. W. Liu, Y. Gao, Y. Guo, F. Zhu, and F.-Y. Wang, "Double domain guided real-time low-light image enhancement for ultra-high-definition transportation surveillance," *IEEE Trans. Intell. Transp. Syst.*, 2024, doi: 10.1109/TITS.2023.3316975.

[11] G. Jocher, A. Chaurasia, and J. Qiu, Ultralytics YOLOv8, ver. 8.0.0, 2023. [Online]. Available: https://github.com/ultralytics/ultralytics. Accessed: Apr. 10, 2026.

[12] M. Safran, A. Alajmi, and S. Alfarhood, "Efficient multistage license plate detection and recognition using YOLOv8 and CNN for smart parking systems," *J. Sensors*, vol. 2024, Art. no. 4917097, 2024, doi: 10.1155/2024/4917097.

[13] A. Ammar, A. Koubaa, W. Boulila, B. Benjdira, and Y. Alhabashi, "A multi-stage deep-learning-based vehicle and license plate recognition system with real-time edge inference," *Sensors*, vol. 23, no. 4, Art. no. 2120, 2023, doi: 10.3390/s23042120.

[14] Z. Cui, "A robust license plate recognition model based on Bi-LSTM," *IEEE Access*, vol. 8, pp. 211630–211641, 2020, doi: 10.1109/ACCESS.2020.3040238.

[15] M. M. Khan, M. U. Ilyas, I. R. Khan, S. Alshomrani, *et al*., "A review of license plate recognition methods employing neural networks," *IEEE Access*, vol. 11, pp. 28646–28674, 2023, doi: 10.1109/ACCESS.2023.3254365.

[16] H. Li, P. Wang, and C. Shen, "Toward end-to-end car license plate detection and recognition with deep neural networks," *IEEE Trans. Intell. Transp. Syst.*, vol. 20, no. 3, pp. 1126–1136, 2019, doi: 10.1109/TITS.2018.2847291.

[17] J. Špaňhel, J. Sochor, R. Juránek, A. Herout, L. Maršík, and P. Zemčík, "Holistic recognition of low quality license plates by CNN using track annotated data," in *Proc. 14th IEEE Int. Conf. Adv. Video Signal Based Surveillance (AVSS)*, 2017, pp. 1–6, doi: 10.1109/AVSS.2017.8078501.

[18] S. M. Silva and C. R. Jung, "License plate detection and recognition in unconstrained scenarios," in *Proc. Eur. Conf. Comput. Vis. (ECCV)*, 2018, pp. 593–609, doi: 10.1007/978-3-030-01258-8_36.

[19] R. Laroca, L. A. Zanlorensi, G. R. Gonçalves, E. Todt, W. R. Schwartz, and D. Menotti, "An efficient and layout-independent automatic license plate recognition system based on the YOLO detector," *IET Intell. Transp. Syst.*, vol. 15, no. 4, pp. 483–503, 2021, doi: 10.1049/itr2.12030.

[20] S. Mittal, "A survey on optimized implementation of deep learning models on the NVIDIA Jetson platform," *J. Syst. Archit.*, vol. 97, pp. 428–442, 2019, doi: 10.1016/j.sysarc.2019.01.011.

[21] C. Chen, Q. Chen, J. Xu, and V. Koltun, "Learning to See in the Dark," in *Proc. IEEE/CVF Conf. Comput. Vis. Pattern Recognit. (CVPR)*, 2018, pp. 3291–3300, doi: 10.1109/CVPR.2018.00347.

[22] M. U. Ramzan, U. Ali, S. H. A. Naqvi, Z. Aslam, Tehseen, H. Ali, and M. Faheem, "Enhancing vehicle entrance and parking management: Deep learning solutions for efficiency and security," *arXiv*, Art. no. arXiv:2312.02699, 2023.

[23] M. A. Hossain, M. S. Kaiser, and M. Mahmud, "A real-time deep learning-based smart surveillance using fog computing: A complete architecture," *Procedia Comput. Sci.*, vol. 218, pp. 1102–1111, 2023, doi: 10.1016/j.procs.2023.01.089.

[24] J. Leng, X. Chen, J. Zhao, C. Wang, J. Zhu, Y. Yan, J. Zhao, W. Shi, Z. Zhu, X. Jiang, Y. Lou, C. Feng, Q. Yang, and F. Xu, "A light vehicle license-plate-recognition system based on hybrid edge-cloud computing," *Sensors*, vol. 23, no. 21, Art. no. 8913, 2023, doi: 10.3390/s23218913.
[25] M. S. Z. Marshoodulla and G. Saha, "SDIoTPark: A data analytics framework for smart parking using SDN based IoT," *IEEE Internet Things J.*, vol. 11, no. 11, pp. 20030–20039, 2024, doi: 10.1109/JIOT.2024.3373133.
[26] NVIDIA, *NVIDIA TensorRT*, 2022. [Online]. Available: https://developer.nvidia.com/tensorrt. Accessed: Apr. 15, 2026.